The Vertical Circulation at Fronts

Objectives

One of the defining structural features of the mid-latitude cyclone is its asymmetric thermal structure manifest most clearly in the fronts that characterize the cyclone. Aside from their ubiquity, these fronts are vested with considerable sensible weather relevance as well since large variations of meteorological conditions exist across them and the precipitation distribution associated with a typical mid-latitude cyclone is often concentrated in their vicinity. Figure 7.1(a) shows analyses of the sea-level pressure and surface potential temperature for a typical mid-latitude cyclone. The characteristic comma-shaped cloud pattern from the same storm (Figure 7.1b) is anchored by the frontal structure identified in Figure 7.1(a). The vigilant reader will be able to establish, through daily inspection of surface, upper air, and satellite observations that the structural relationship demonstrated in Figure 7.1 is quite common in the middle latitudes.

Note that the across-front dimension of the cold front in Figure 7.1(a) (on the order of 100 km) is much smaller than its along-front dimension (on the order of 1000 km). Considering characteristic velocities given such length scales we can draw the preliminary conclusion that geostrophic balance exists in the along-front direction (where the Rossby number (R_o) is given by $R_o = 10 \, \mathrm{m \, s^{-1}}/(10^{-4} \, \mathrm{s^{-1}})(10^6 \, \mathrm{m}) = 0.1$. However, in the across-front direction $R_o = (10 \, \mathrm{m \, s^{-1}})/(10^{-4} \, \mathrm{s^{-1}})(10^5 \, \mathrm{m}) = 1.0!$ Thus, mid-latitude fronts would appear to be hybrid phenomena characterized by along-front geostrophy but a fair degree of across-front ageostrophy. The mixture of scales that characterizes fronts makes them the focus of important scale interactions in the mid-latitude cyclone. For this reason, the purely quasi-geostrophic diagnostic perspective we have thus far developed will prove to be insufficient as a means to investigate fronts and it will have to be extended in order to incorporate additional, physically relevant processes that are fundamental to the frontal environment.

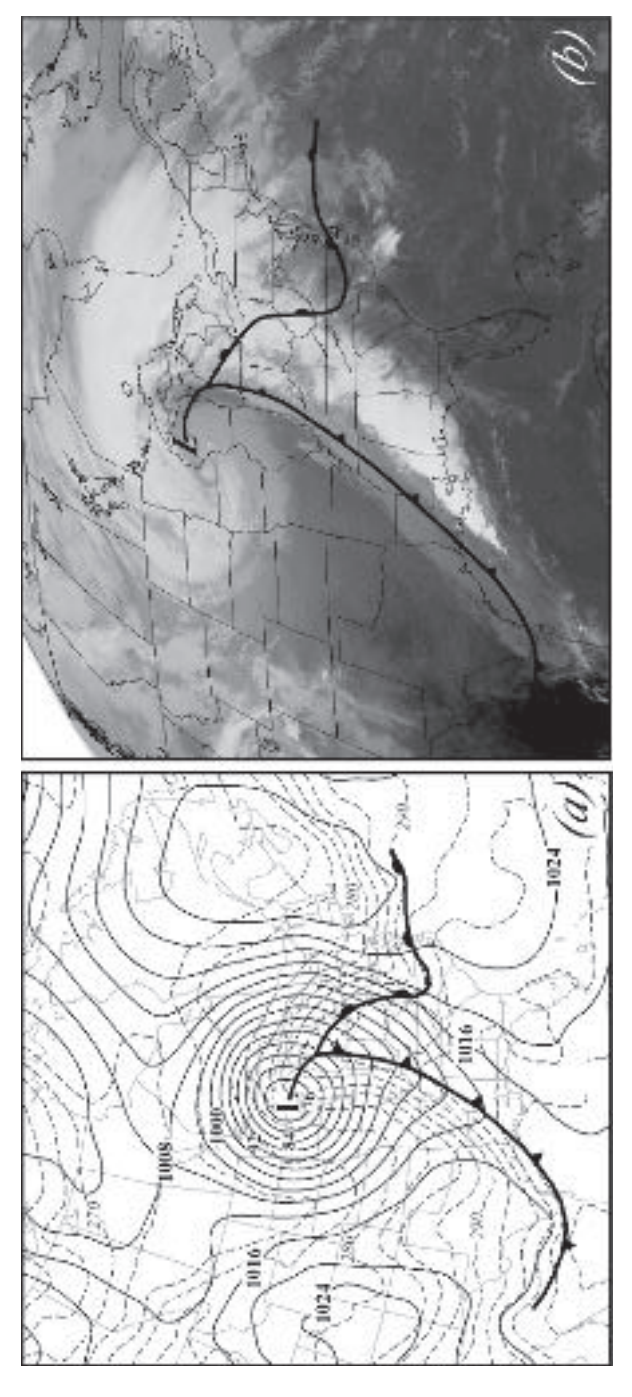


Figure 7.1 (a) Sea-level pressure and 950 hPa potential temperature analysis at 1800 UTC 10 November 1998. Solid lines are sea-level isobars, labeled in hPa and contoured every 4 hPa. Dashed lines are 950 hPa isentropes labeled in K and contoured every 2.5 K. Standard frontal symbols identify the cold and warm fronts while the occluded front is indicated as a thick black line. (b) Infrared satellite image (NOAA) of the same storm at 1815 UTC 10 November 1998. Frontal symbols as in (a)

Given the relationship between fronts and the cloud and precipitation distribution in mid-latitude cyclones that is suggested by Figure 7.1, a central question for our subsequent investigation is: *Why is such a relationship so prevalent?* In order to approach this question with precision, we first need to understand the essential elements of frontal structure. Next we consider how **frontogenesis**, the process of creating a front, leads to the vertical motions that characterize fronts. Adoption of a *semi-geostrophic* perspective in the Sawyer–Eliassen frontal circulation equation formally incorporates the interplay between the geostrophic and ageostrophic flows that characterizes the frontal environment. We then proceed to an investigation of fronts that form at the tropopause, known as upper-level fronts. Finally we consider some of the circumstances that conspire to produce the observed variation of precipitation intensity associated with fronts. We begin by establishing the essential characteristics of fronts in the next section.

7.1 The Structural and Dynamical Characteristics of Mid-Latitude Fronts

As demonstrated by Figure 7.1(a), a front is a boundary whose primary structural and dynamical characteristic is the larger-than-background temperature (or density) contrast associated with it. In order to determine some basic characteristics of fronts, from which we will create a working definition of a front, we will consider the somewhat unphysical case of the **zero-order front**. The zero-order front is characterized by *discontinuities* in the temperature and density across the frontal boundary. For this reason, it most closely approximates the notion of the knife-like polar front envisioned by the Bergen School in the Norwegian Cyclone Model. Real fronts, however, actually more closely resemble a first-order front, in which *gradients* of temperature and density, not the variables themselves, are discontinuous across the front. Since a front is a boundary between two different air masses and each air mass has a characteristic density, in a zero-order front density is discontinuous across the front (Figure 7.2). We will demand that pressure be continuous across

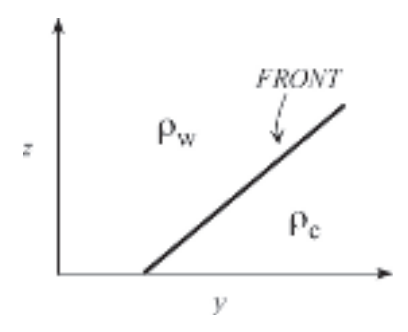


Figure 7.2 Vertical cross-section through the zero-order front

the zero-order front (so that the geostrophic winds are not infinite along the front!). Then, according to the gas law, temperature (T) must also be discontinuous across the front. Even though this will imply an infinite thermal wind, we will proceed anyway, the simplicity of the ensuing analysis being the motivation. If we take the x-axis as the along-front direction and further assume (1) that there is no along-front variation in any variable, and (2) that the pressure is steady state (i.e. $\partial p/\partial t = 0$), then the differential of pressure is given by

$$dp = \left(\frac{\partial p}{\partial y}\right) dy + \left(\frac{\partial p}{\partial z}\right) dz \tag{7.1}$$

on both sides of the front. This expression can be written for both the warm and the cold sides of the front as

$$dp_w = \left(\frac{\partial p}{\partial y}\right)_w dy + \left(\frac{\partial p}{\partial z}\right)_w dz$$
 and $dp_c = \left(\frac{\partial p}{\partial y}\right)_c dy + \left(\frac{\partial p}{\partial z}\right)_c dz$,

respectively. We can use the hydrostatic equation to substitute for $\partial p/\partial z$ in both expressions, set the expressions for dp equal to one another, and rearrange the result to get

$$0 = \left[\left(\frac{\partial p}{\partial y} \right)_c - \left(\frac{\partial p}{\partial y} \right)_w \right] dy - (\rho_c - \rho_w) g dz. \tag{7.2}$$

This can be solved for dz/dy, the slope of the zero-order front:

$$\frac{dz}{dy} = \frac{(\partial p/\partial y)_c - (\partial p/\partial y)_w}{g(\rho_c - \rho_w)}.$$
 (7.3)

Since more dense fluid must lie beneath less dense fluid, as portrayed in Figure 7.2, in order that the frontal structure be statically stable and therefore sustainable, we note that dz/dy>0. From (7.3), this implies that the across-front pressure gradient must be larger on the cold side of the front than on the warm side. Such a conclusion can be incorporated into constructing a physically accurate analysis of sea-level pressure in the vicinity of a front. Perhaps more enlightening for our investigation is to consider the along-front geostrophic winds which are related to the across-front pressure gradients. Recall that, in height coordinates,

$$u_g = -\frac{1}{\rho f} \frac{\partial p}{\partial y}$$
 or $\frac{\partial p}{\partial y} = -f \rho u_g$.

Using this expression we can recast (7.3) into

$$\frac{dz}{dy} = \frac{f(\rho_w u_{g_w} - \rho_c u_{g_c})}{g(\rho_c - \rho_w)}.$$
(7.4)

Now, in order for dz/dy > 0 we see that $u_{g_w} > u_{g_c}$; in other words, the front must be characterized by positive geostrophic relative vorticity $(\partial u_g/\partial y < 0)$! Thus, we

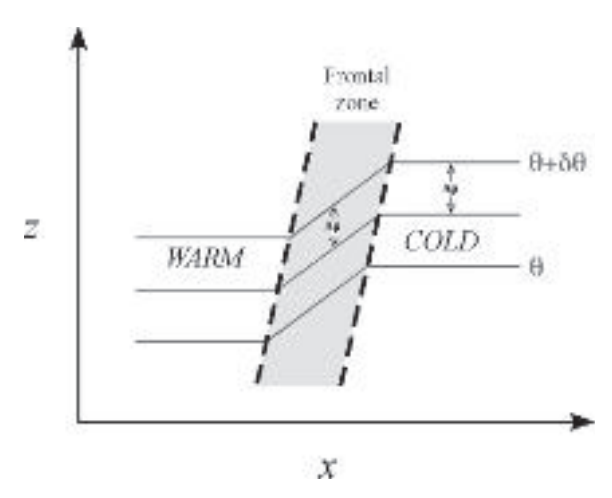


Figure 7.3 Isentropes associated with a first-order front. Note that the static stability is largest in the frontal zone

have discovered a fundamental dynamical characteristic of mid-latitude fronts – they are characterized by positive geostrophic relative vorticity. In fact, further inspection of (7.4) reveals that the stronger the density contrast across the front becomes, the more intense is the vorticity at the front.

In reality, the temperature cannot be discontinuous at a front, but the temperature gradient can be. In this more realistic case, we have a first-order discontinuity and the isentropes must appear as in Figure 7.3 in the first-order front. Careful examination of the isentropes in the frontal zone reveals that the frontal zone is also characterized by larger static stability $(-\partial\theta/\partial p)$ than either the cold or warm side of the boundary. Thus, frontal zones are characterized by (1) larger-than-background horizontal temperature (density) contrasts, (2) larger-than-background relative vorticity, and (3) larger-than-background static stability. We will use these characteristics to define a front after we examine some observations of fronts.

A time series of rooftop observations at Madison, Wisconsin (known as a meteorogram) is shown in Figure 7.4(a). Note the $\sim 5^{\circ}\text{C}$ drop in temperature and corresponding 3°C drop in dewpoint temperature that occurred between 0510 and 0515 UTC. Simultaneously, the winds shifted from steady southwesterlies to steady northerlies. This time series clearly demonstrates the sharp temperature and moisture characteristics associated with a surface frontal passage (in this case, a cold frontal passage). It also reveals the strong cyclonic vorticity that must attend a midlatitude frontal zone. Evidence for the enhanced static stability of a frontal zone is provided in Figure 7.4(b) which is a vertical cross-section through what is known as an upper-level front. Note that the static stability is elevated in the stratosphere, as expected, but also within the bundle of isentropes that extends beneath the jet maximum to nearly 700 hPa. This same bundle of isentropes constitutes the upper

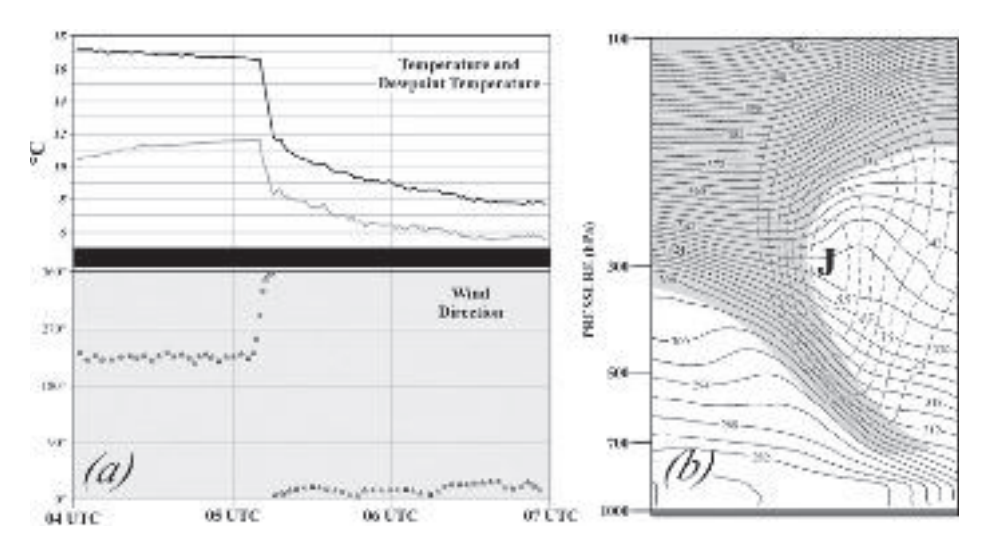


Figure 7.4 (a) Meteorogram of a surface cold frontal passage at Madison, WI between 0400 and 0700 UTC 30 April 2003. Black line is the temperature, gray line is the dewpoint, and asterisks are the wind direction time series, respectively. Note the coincidence of the temperature and dewpoint drops with the wind shift. (b) Vertical cross-section through an upper-level frontal zone at 1200 UTC 12 November 2003. Solid lines are isentropes labeled in K and contoured every 3 K. Dashed lines are isotachs labeled in m s⁻¹ and contoured every 10 m s⁻¹ starting at 25 m s⁻¹. Gray shading represents region of enhanced static stability which includes the upper-frontal zone itself

front itself and is clearly characterized by large horizontal temperature contrast as well as cyclonic vorticity (evidenced by the horizontal shear implied by the tight packing of the isotachs). Now we are prepared to establish a working definition of a front that is based upon the essential characteristics of mid-latitude frontal zones. When we use the term 'cold (warm) front' we will be referring to:

The leading edge of a transitional zone that separates advancing cold (warm) air from warm (cold) air, the length of which is significantly greater than its width. The zone is characterized by high static stability as well as larger-than-background gradients in temperature and relative vorticity.

In nature, fronts defined in this way come in varying degrees of intensity but every front shares these fundamental physical and dynamical characteristics. Thus, the lack of a numerical designation here is not an oversight but rather an attempt to distinguish those features in the mid-latitude atmosphere that ought to be called fronts from those which should not. Of course, the intensity of a front *is* a meaningful distinction to make in terms of both scientific interest as well as sensible weather characteristics. One way of measuring the strength of one front against another is by considering the *magnitudes* of their respective horizontal temperature gradients. We will return to this important diagnostic in just a moment. First we will consider the intimate relationship between fronts and jets in the mid-latitude atmosphere.

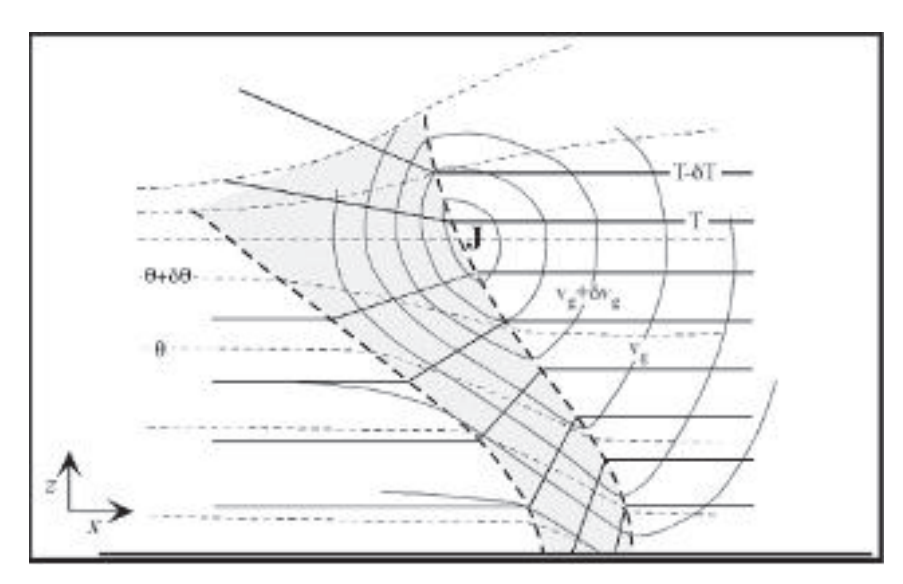


Figure 7.5 Idealized vertical cross-section through a frontal zone. Gray solid lines are isotachs of the geostrophic wind into the page with 'J' indicating the position of the wind maxima. Black solid lines are isotherms and thin dashed lines are isentropes. Gray shaded region with thick dashed border represents the idealized frontal zone

7.2 Frontogenesis and Vertical Motions

The thermal wind relation requires that fronts (regions of large ∇T) be associated with strong vertical shear of the geostrophic wind. Shown in Figure 7.5 is an idealized vertical cross-section through a frontal zone. Notice that the magnitude of ∇T is largest near the surface and that the frontal zone is characterized by the strongest vertical shear. Also notice that the leading edge of the zone (i.e. the front itself) is a maximum in geostrophic relative vorticity as we have previously suggested it should be. Recall from the frictionless vorticity equation that vorticity can change only as a result of divergence $(d\eta/dt = -f(\nabla \cdot \vec{V}))$. By the continuity equation, divergence is accompanied by vertical motions $(\nabla \cdot \vec{V} = -\partial \omega/\partial p)$. Using these two relationships we can establish the following logical argument. If, by some horizontal advective process, for instance, the magnitude of ∇T increases, then the wind shear and jet core wind speed necessarily increase as well. A more intense jet results in increased vorticity. Increased vorticity implies that some divergence is operating in the fluid. If divergence is operating, there must be some vertical motion as well. Therefore, an increase in the magnitude of ∇T requires the production of a vertical circulation in an atmosphere in approximate thermal wind balance. For the remainder of this chapter we will investigate various physical/mathematical formulations that seek to quantify this important physical relationship. The first step on this journey requires that we consider how an increase in the magnitude of ∇T can be accomplished.

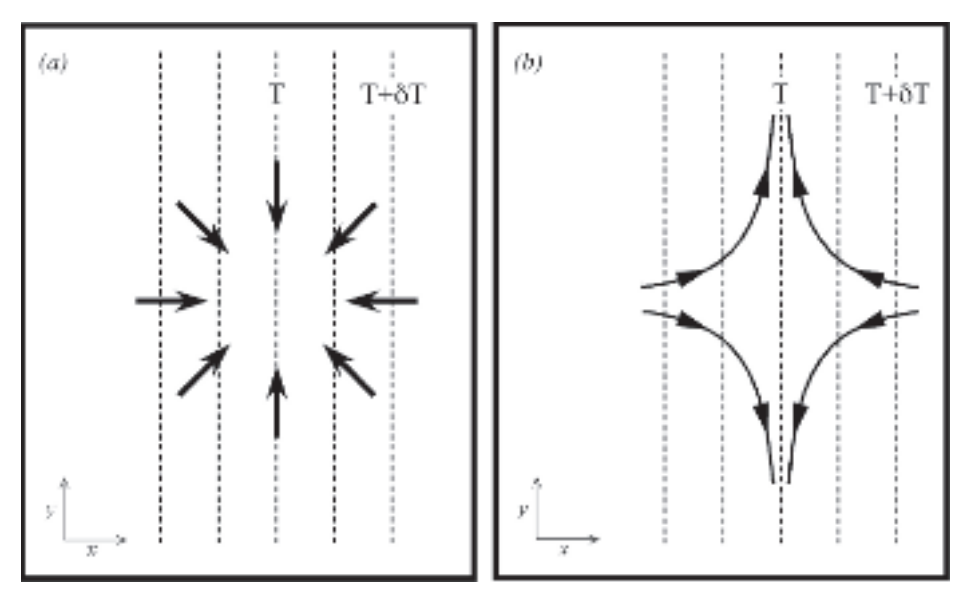


Figure 7.6 (a) Pure convergence superimposed upon a field of isotherms. (b) Horizontal deformation superimposed upon a field of isotherms. In both cases the horizontal wind will tend to intensify $|\nabla T|$

We shall broadly define as 'frontogenetic' any process that acts to increase the magnitude of ∇T . Such a process in action is known as **frontogenesis**. More specifically (for ease of physical interpretation later), we will refer to any horizontal advective process that acts to increase the magnitude of ∇T as **horizontal frontogenesis**. Some simple illustrations of horizontal frontogenetical processes are given in Figure 7.6. Given our verbal definition of frontogenesis, we can define a corresponding mathematical one (termed the **frontogenesis function**) as

$$\Im = \frac{d \left| \nabla_p \theta \right|}{dt},\tag{7.5}$$

defining the Lagrangian rate of change of the magnitude of $\nabla_p \theta$ (the potential temperature gradient measured on an isobaric surface). Though it looks innocuous, (7.5) is a rather bulky expression (as we will see presently). Without loss of physical insight, we can consider the simpler 1-D version of (7.5) and gain some understanding of the nature of frontogenesis. Therefore, we will consider the processes that can change the magnitude of the *x*-direction temperature contrast using

$$\Im_x = \frac{d}{dt} \left(\frac{\partial \theta}{\partial x} \right).$$

The reader is asked to show that, given

$$\frac{d}{dt} = \frac{\partial}{\partial t} + u \frac{\partial}{\partial x} + v \frac{\partial}{\partial y} + \omega \frac{\partial}{\partial p},$$

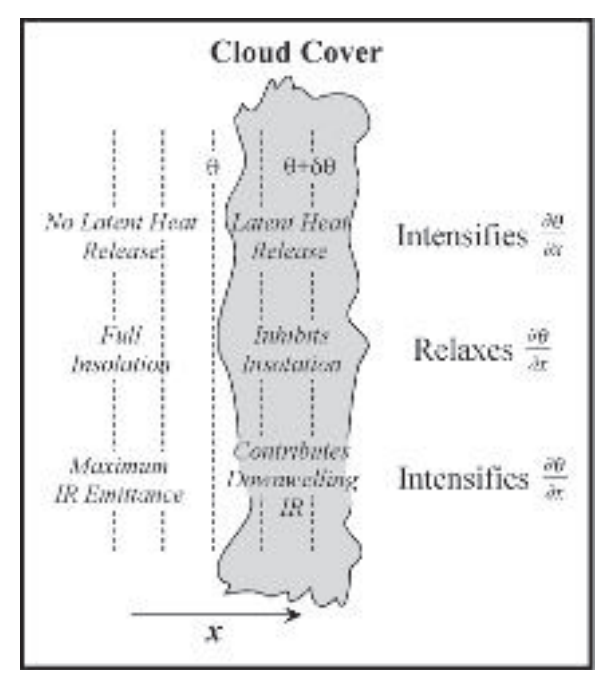


Figure 7.7 The diabatic effects of cloud cover on $\partial\theta/\partial x$. The effect of differential latent heat release can occur at any time of day. Differential insolation and infrared emittance are specific to day and night, respectively

then

$$\Im_{x} = \frac{d}{dt} \left(\frac{\partial \theta}{\partial x} \right) = \frac{\partial}{\partial x} \left(\frac{d\theta}{dt} \right) - \frac{\partial u}{\partial x} \frac{\partial \theta}{\partial x} - \frac{\partial v}{\partial x} \frac{\partial \theta}{\partial y} - \frac{\partial \omega}{\partial x} \frac{\partial \theta}{\partial p}. \tag{7.6}$$

Thus, there are four physical processes, represented by the four terms on the RHS of (7.6), that contribute to an increase in $\partial\theta/\partial x$. The first of these processes is the effect of across-front gradients in diabatic heating, represented by $\partial/\partial x(d\theta/dt)$. Consider the meridionally oriented isentropes illustrated in Figure 7.7. If there is latent heat release in ascending air on the warm side of this potential temperature gradient, then $\partial/\partial x(d\theta/dt) > 0$. Consequently, such a distribution of latent heat release is frontogenetical. Utilizing the same expression we can consider the effect of differential cloud cover on frontal strength. If the warm side of Figure 7.7 is cloudy and the cold side clear, then differential insolation during the day renders $\partial/\partial x(d\theta/dt) < 0$ and daytime heating is frontolytic under such circumstances. Under the same distribution of clouds during the night, the cold side cools more rapidly than the warm side so that $\partial/\partial x(d\theta/dt) > 0$ and so the cloud cover promotes frontogenesis.

The effect of confluence over the temperature gradient is represented by the second term on the RHS of (7.6),

$$-\frac{\partial u}{\partial x}\frac{\partial \theta}{\partial x}$$
.